JOURNAL OF SPACECRAFT AND ROCKETS
Vol. 29, No. 2, March-April 1992

Flow in a Model of the Space Shuttle Main Engine Main Injector Bowl

B. E. Thompson* and J. Senaldi†
Scientific Research Associates, Inc., Glastonbury, Connecticut 06033
C. Vafidis‡ and J. H. Whitelaw§
Imperial College, London, England, SW7 2BX, United Kingdom
and
H. McDonald¶
Scientific Research Associates, Inc., Glastonbury, Connecticut 06033

Velocity measurements and flow visualization were obtained in a specially prepared 32% model of the Space Shuttle main engine (SSME) main injector bowl. Refractive-index-matching techniques were used to obtain three components of mean and fluctuating velocities throughout the flow without the usual restrictions associated with multiple solid-liquid boundaries and complex surface curvature. Measurements of mean-flow and turbulence normal stresses were obtained to quantify flow characteristics in the inlet ducts, entrance region, racetrack, LOX postbundle, and exit nozzle. Measured velocity distributions show the upstream effect of the injector bowl in the transfer ducts, the plenum effect of the racetrack and LOX postbundle, and the nonuniform distribution of the flow into the main exit nozzle.

Nomenclature

D = duct diameter, m
n = index of refraction
R_e = Reynolds number, UD/ν
T = temperature, °C
U = velocity, m/s
U_B = bulk velocity, Q/A, m/s
x,y,z = coordinate direction (see Fig. 1), m
ν = kinematic viscosity, m^2/s
ρ = density, kg/m^3

Subscripts

E = exit plane of nozzle
H = LH_2-side transfer duct
m = matching
x,y,z = coordinate directions (see Fig. 1)
$< >$ = time-averaged value

I. Introduction

REFRACTIVE-INDEX-MATCHING techniques have been developed to allow laser-velocimetry measurements in the flow through complex geometries. The measurement of internal flows confined by complex boundaries is often restricted by accessibility difficulties. These may be due to flow interference when using probes in narrow flow passages or to access restrictions imposed by the geometry of the model boundaries when using optical measurement techniques. The nonintrusive nature of laser velocimeters, combined with their insensitivity to fluid properties and flow conditions, renders their use particularly attractive for the study of complex flow configurations, provided that adequate optical access can be attained. The use of optically flat windows or transparent models may provide the necessary optical access in many flow configurations but in some cases the presence of multiple solid boundaries and complex surface curvatures poses added measurement limitations. These difficulties arise from differences in refractive indices of the fluid and the model material along the path of the laser beams whose intersection forms the measurement volume of the laser velocimeter. These refractive-index differences may affect the measurement position and sensitivity factor of the laser velocimeter, and in many cases prevent any measurement because the laser beams will not intersect to form an interference measurement volume. It is on this latter observation that the principle of refractive index matching is based.

Early application of refractive index matching in laser-velocimetery measurements concentrated on a simple circular duct flow with emphasis on near-wall regions.[1] The conclusion was that disturbance-free measurements in the near-wall region of the pipe were possible using the refractive-index-matching techniques, and the results were in agreement with theoretical results derived from the momentum equations. Measurements as close as 300 μm from the wall were obtained as opposed to 1-1.5 mm when using conventional hot-wire or hot-film sensor probes. The liquid used to match the refractive index of the glass wall was a mixture of light fuel oil and dibutylphthalate. The resulting mixture matched the refractive index of the glass within n of 10^{-4} but its viscosity was higher than that of water. A number of suitable fluids and mixtures to match the refractive index of glass were also examined in Ref. 1 and classified according to toxicity, chemical aggressivity, and flammability. In general, these fluids were organic solvents, not suitable for use with acrylics.

Another early application[2] of refractive index matching concentrated on velocity field measurements in a rod bundle and between cylindrical roughness elements in boundary layers. Most of the optical boundaries were made of glass and

Received Jan. 13, 1990; revision received Oct. 15, 1990; accepted for publication May 14, 1991. Copyright © 1990 by Scientific Research Associates, Inc. Published by the American Institute of Aeronautics and Astronautics, Inc., with permission.

*Supervisor, Experimental Gas Dynamics, 50 Nye Road, P.O. Box 1058; currently Associate Professor, Department of Mechanical Engineering, Aeronautical Engineering, and Mechanics, Rensselaer Polytechnic Institute, Troy, NY 12180. Member AIAA.
†Associate Research Scientist; currently Engineer, General Electric, Milwaukee, WI.
‡Research Fellow, Fluids Section, Exhibition Road.
§Professor of Convective Heat Transfer, Department of Mechanical Engineering, Exhibition Road.
¶President, 50 Nye Road, P.O. Box 1058. Member AIAA.

the matching fluids were primarily mineral and silicon oils. This resulted in high viscosities and, thus, typical Reynolds numbers for these experiments were in the laminar regime. In addition, the manufacture of complex models from glass is difficult.

The approach taken here is to use laser velocimetry in a mixture of organic solvents flowing through acrylic models. The fluid is a 70%/30% mixture of oil of turpentine and 1,2,3,4-tetrahydronaphthalene (Dupont Tetralin) matched to the refractive index of the cast acrylic at a specified temperature. Reference 3 examined a number of converging swirl chambers and used this approach to enable detailed scanning of the flowfield, despite irregularities in flow boundaries. This solution is preferred here because it combines low toxicity with reasonable cost, and it has low viscosity so that Reynolds numbers can be arranged to correspond to those of turbulent flow. Its main disadvantages are associated with fumes when leaks occur and the finite life of models due to chemical degradation. Clear-cast acrylics have excellent machinability and transparency, and it is an excellent choice of materials for construction of models. However, the surface of these models is vulnerable to chemical attack from the turpentine-Tetralin solution so that softening and crazing can occur: current practices result in a model life of about 26 months.

The present refractive-index-matching technique has been used in previous investigations of complex flows,[5-8] flows with rotating components,[9] and two-phase flows.[4,10-14] This approach allowed measurement with high Reynolds numbers and inexpensive models. The flowfield behind a confined disc in a circular duct[8] has been studied using refractive-index-matching techniques and the results were compared to those[15] obtained in airflow and were found to be in very good agreement. Accurate velocity measurements in two-phase flows with high particle concentration were demonstrated,[9] following feasibility and preliminary studies,[11,12,14] and are based on matching the refractive index of the transparent solid particles, thus minimizing their effect on the laser-beam path. This technique was also used for single- and two-phase flow measurements around the transparent blades of a chemicals mixer[9,13] and for the mapping of the steady flowfield inside a transparent model of a directed port of an internal combustion engine.[6,7] Another favorable application was in the flow through rod bundles of heat exchangers, with emphasis on the flow-induced vibrations of the rods.[8]

This paper presents mean-flow and turbulence quantities obtained in a 32% acrylic model of the Space Shuttle main engine (SSME) main injector bowl. The flow structure through the bowl, ducts, and rod bundle is not well-understood and there is concern that flow-induced vibrations may affect the durability of the SSME powerhead. It is likely that this type of injector bowl structure will be used in future compact and advanced rocket-engine configurations and, accordingly, knowl-

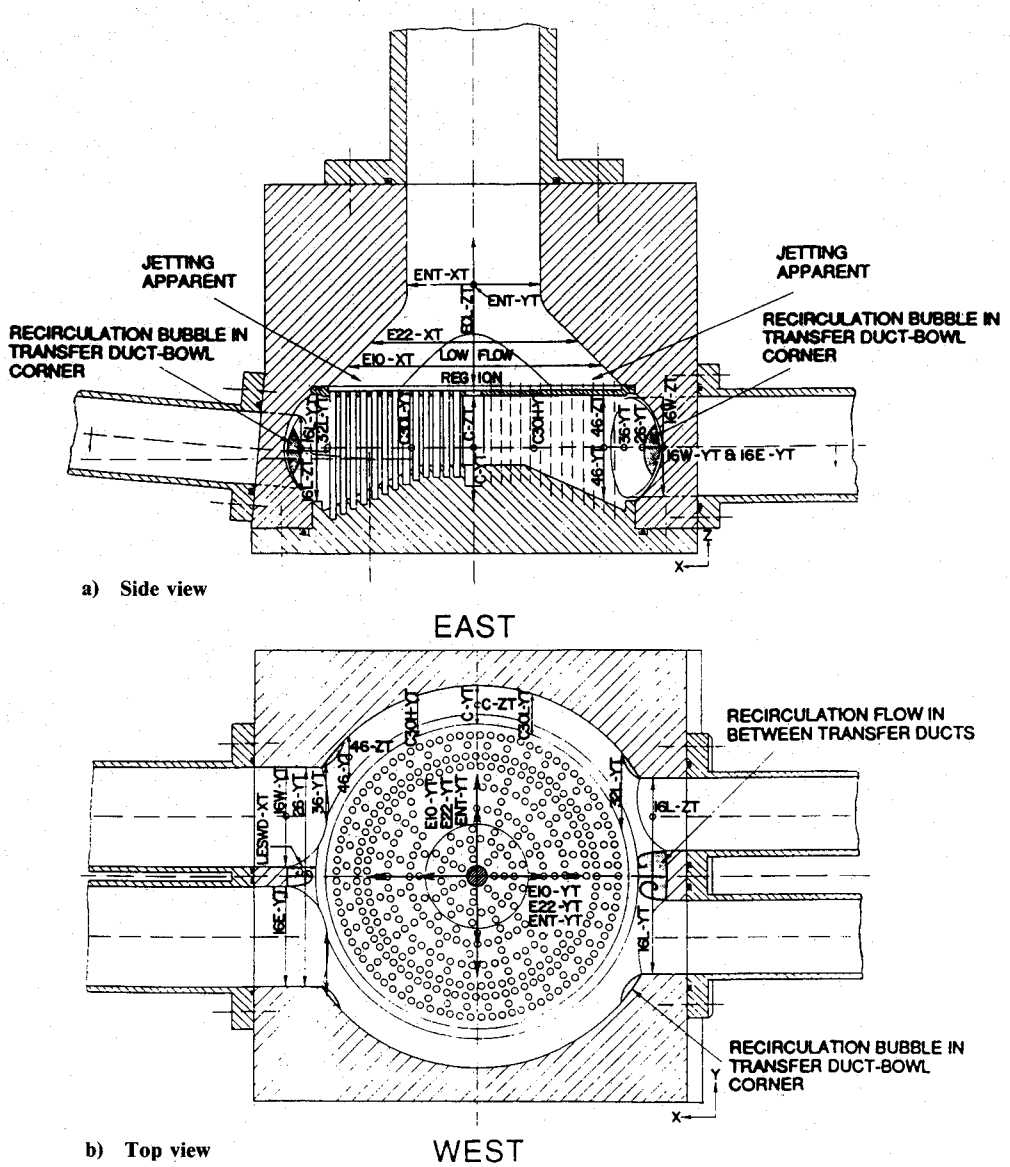

Fig. 1 Measurement locations and flow features.

edge and procedures will be needed for design purposes. The present results contribute fluid mechanics understanding and provide detail adequate for validation of computational design procedures in relevant geometry. The developed refractive-index-matching technique also provides capability for future investigation of similar complex internal flow configurations.

The flow configuration and refractive-index-matching approach are described in Sec. II. Section III describes the flow visualization and laser-velocimetery instrumentation. This is followed in Sec. IV by presentation and discussion of the flow patterns and velocity results. The paper ends with concluding remarks about both the present refractive-index-matching technique and the flow phenomena found in the model of the SSME main injector bowl.

II. Flow Configuration

Figure 1 shows the 32%-scale model of the present study that comprises two pairs of inlet ducts, a bowl-shaped mixing chamber, a bundle of 464 rods representing LOX posts, and an outlet nozzle. The model is a cast acrylic version of the water-test Model No. 517 (two-duct) assembly that is half-scale of the actual SSME main engine. A detailed comparison of the 32% model and the SSME configuration is given in Ref. 5. The external shape of the 32% model is rectangular to provide a simple optical interface and, thus, excellent optical accessibility.

Solid acrylic has an index of refraction of 1.4893 at 23.4°C for light at 632.8 nm, and this is between the refractive index of steam-distilled turpentine and Tetralin, which are about 1.468 and 1.546, respectively. Accordingly, a mixture of these liquids can be prepared to match the refractive index of the acrylic and depends on mixture concentration and temperature. Many combinations of concentration and temperature can provide a match and the practice recommended here is to operate with about a 30% Tetralin concentration and to fine tune the temperature setting to match the refractive indices. This concentration was chosen to give a matching temperature slightly above ambient because, first, high temperatures will shorten model life, second, cooling systems can be expensive and, last, a finite temperature difference will reduce the time constant of the temperature control feedback loop. Table 1 gives the characteristics of the fluid used here.

The above model was arranged in the refractive-index-matching flow circuit, which comprised a holding tank, two pumps, two sets of inlet transfer duct pairs with flow control valves, the model, and a single return duct to the holding tank. The holding tank contained heating and cooling elements that were operated by a feedback controller (West 2070 Microprocessor-based PID controller) in order to keep the fluid at a constant preselected temperature that matched refractive indices of the acrylic and fluid within n of 0.0001. The fluid temperature at the exit of the model was obtained from a platinum-film thermistor. Stainless-steel rotameters (Aquamatic FLT-4-32 and FLT-4-50) were used to monitor the flow rate in each transfer duct within 1% and were located upstream of the inlet pipes that extended 20 diameters upstream of their entrance to the model and resulted in swirl-free, fully developed, turbulent flow at the model inlet. A strainer (Rosedale 4-6-1-200-D-S316-T-S-M200) was incorporated into the flow circuit to limit the maximum seed particle size to 2-μm diam. Two stainless-steel pumps with Teflon seals and explosion-proof motors (Price SC-100-33 and SC-150-150 pump assemblies) were used to provide the LH2-side and LOX-side flow with a nominal flow split of 70–30%, respectively. Table 2 provides the operating conditions, Reynolds numbers, and characteristic dimensions.

III. Instrumentation

Flow visualization was obtained with laser sheets and with conventional photographic techniques. Small air bubbles were created in the solution to scatter light and visualize the flow patterns. The bubbles were formed by mixing air with the solution in the holding tank and allowing the pumps to break any large bubbles into a uniform distribution of about 0.5-mm-diam bubbles. The number of bubbles was controllable and arranged so that the flow patterns could be seen for photographic purposes.

A dual-beam, single-component laser velocimeter[16] was used in a forward-scatter configuration to obtain the present results. A 5-mW helium-neon-laser was focused on a rotating diffraction grating and the two first-order beams transmitted and focused inside the SSME model to provide an appropriate interference volume. The dimensions of the volume, the fringe spacing, the range of frequency shift, and other details of the optical characteristics of the laser velocimeter are shown in Table 3. Frequency shift was needed and used to resolve reverse velocities in the vicinity of recirculating flow. The signal-processing system was based on a Doppler-burst frequency counter interfaced to a microcomputer for data acquisition and processing. Measurements were obtained with the collection optics arranged in on-axis and off-axis, forward-scatter mode and also in an off-axis, back-scatter configuration depending on the optimum signal-to-noise ratio. Seeding for the laser velocimeter was with Teflon particles smaller than 2-μm diam and with particle arrival rates such that temporal resolution was limited by the cycle time of the counter instrumentation.

Maximum experimental uncertainties for the mean velocities and Reynolds normal stresses were 2 and 5% of the local value based on the above optical and processing configuation. Mean flow rates were monitored to within 1% and the temperature of the refractive-index-matching fluid was held constant within 0.1°C. The transmission and collection optics were mounted on a mechanism that traversed the measurement vol-

Table 1 Properties of the refractive-index-matching fluid

Density	ρ = 893 kg/m^3
Viscosity	ν = 1.74 × 10^{-6} m^2/s
Refractive index	n = 1.4897 @ 632.8 nm
Matching temperature	T_m = 26.1°C

Table 2 Operating conditions and characteristic dimensions

Volume flow rate (each duct balanced)	
LH_2-side duct	27.3 USGPM
LOX-side duct	11.6 USGPM
Overall	77.8 USGPM
Bulk mean velocity	
LH_2-side duct, U_{BH}	0.994 m/s
Exit of nozzle, U_{BE}	1.425 m/s
Reynolds number	
LH_2-side transfer ducts	27,000
LOX-side transfer ducts	15,700
Exit of nozzle	54,900
Diameter	
LH_2-side transfer duct, D_H	47.5 mm
LOX-side transfer duct	35 mm
Exit nozzle, D_E	67 mm
Lox posts	3 mm

Table 3 Optical characteristics of the laser velocimeter

Half angle of the beam intersection, deg	5.97
Fringe spacing	3.04
Number of fringes without frequency shift	27
Diameter of the control volume at $1/e^2$ intensity, μm	81
Length of the control volume at $1/e^2$ intensity, μm	774
Maximum frequency shift, MHz	±3
Frequency to velocity conversion, ms^{-1}/MHz	3.04

ume in three directions with a maximum positional uncertainty less than 0.02 mm (0.001 in.).

IV. Results and Discussion

Velocity measurements and flow visualization were obtained in the specially prepared model of the SSME main injector bowl. Tabular data[17] are available for comparison to the calculations. Flow visualization showed a strong interaction of LOX- and LH_2-side flows in the racetrack but suggested a more uniform outlet flow, although jetting was apparent in the near field of the exit plane from the LOX postbundle. Figure 1 shows the major flow features including dimensions of the recirculation regions in the following locations: in the entrance regions between the inlet of transfer ducts; downstream of the sharp corners where the transfer ducts join the injector bowl; and in the central core of the exit nozzle. The first two of these recirculations were induced by sharp backward-facing corners.

Measurements of mean-flow and turbulence quantities were obtained with laser velocimeter and confirm the above results. Flow characteristics in the inlet ducts, entrance region, racetrack, LOX postbundle, and exit nozzle were obtained at the locations shown in Fig. 1 with the objective of providing understanding and allowing validation of calculation methods.

Figure 2 shows distributions of mean-flow velocity in the LH_2-side transfer ducts and entrance region of the main injector bowl. The inlet pipe flow was measured to be fully developed, turbulent, and swirl-free. The influence of the injector

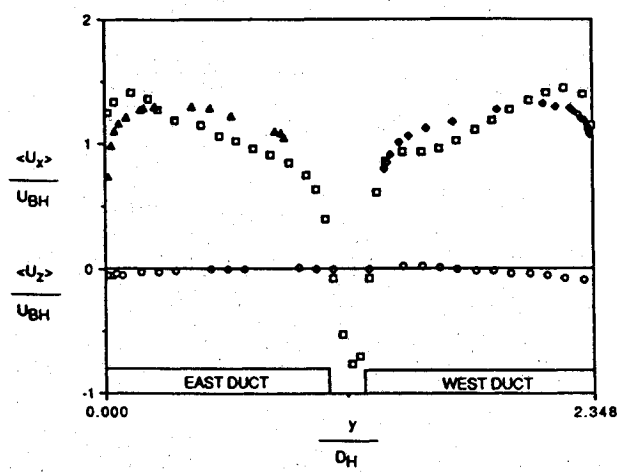

Fig. 2 Mean velocity distribution in the region of the LH_2-side transfer ducts and entrance to the main injector bowl (△ $<U>$ at 16E-YT; □ $<U>$ at 26-YT; ◇ $<U>$ at 16W-YT; and ○ $<W>$ at 26-YT).

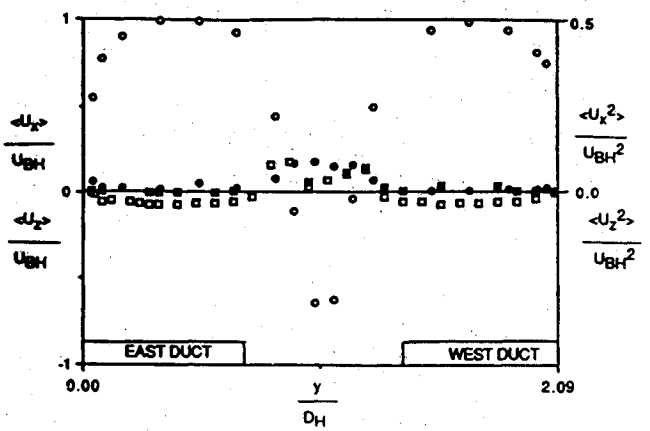

Fig. 3 Velocity characteristics in LOX-side entrance region at 16L-YT (□ $<W>$ mean velocity; ○ $<U>$ mean velocity; ■ $<W>$ turbulence normal stress; and ● $<U>$ turbulence normal stress).

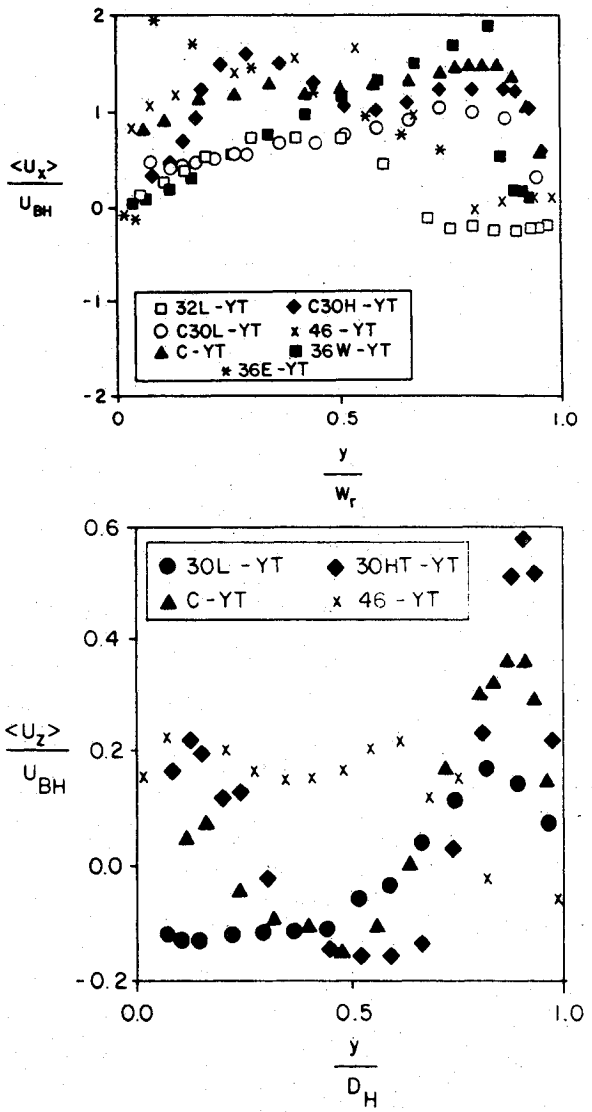

Fig. 4 Velocity distribution in the racetrack: a) X component of mean velocity; and b) Z component of mean velocity.

bowl and LOX postbundle is apparent on the distribution of mean velocity in the inlet ducts upstream of the entrance to the racetrack. A similar effect was observed[18] in measurements obtained in a similar water model of the SSME powerhead. In that flow, the geometry simulated flow from the turbine exit downstream to the exit nozzle and comprised a turn-around duct, one pair of transfer ducts, a simplified injector bowl, and an exit nozzle; there were no internal posts in the injector bowl and, accordingly, the flow patterns in this region and in the exit nozzle were considerably different than those of the present experiment. Also, there was substantial streamwise vorticity in previous transfer duct flow[18] that was generated as the flow turned from the turn-around duct into the transfer ducts. Velocity measurements[18] showed effects upstream of the injector bowl on flow in the transfer ducts and the magnitude in the mean velocity distribution was similar to that found here. This is somewhat noteworthy considering differences in these flow configurations and may be attributed in part to the pressure-driven nature of the flow in the entrance region.

Recirculating flow is apparent in Fig. 2 downstream of the divider between the transfer ducts. Vortex shedding at a frequency of about 10 Hz was apparent during flow visualization downstream of the gap between the LH_2-side transfer ducts. An unsteady vortex core was visible in the recirculating flow between the transfer ducts shown in the flow visualization of

Fig. 1, and it precessed over about a 10-mm diam at the centerline of the racetrack and over about a 3-mm diam close to the racetrack walls. In the mean, it was aligned with the exit nozzle axis except within about 0.1 LH_2-side duct diameter of the racetrack wall. Turbulence normal stresses were large in the vicinity of this recirculation as is expected with large shear stress production associated with backflow.

Figure 3 shows velocity distributions in the LOX-side entrance region and these are similar to those of the LH_2 side in the following manner: the central recirculation region between the transfer ducts is again present, the z-direction distributions have modified pipe-flow characteristics, and the crossflow, z-direction component of velocity is again small.

Mean velocity distributions in the racetrack is shown in Fig. 4. Turbulence quantities[17] are large but without unusual features. Recirculation regions are apparent downstream of the sharp corner where the transfer ducts meet the injector bowl. This recirculation bubble extends across about 60% of the transfer duct diameter and its small streamwise dimensions of about $0.2D$ suggests that smooth fairing of the transfer duct to the injector bowl, as is in current use on the SSME, would not induce separation. In the upstream region of the racetrack on the LH_2 side, the mean velocity distribution increases linearly from the LOX postshields to the outer racetrack wall as is indicative of a forced vortex. This linear structure changes along the racetrack as flow escapes through the LOX postbundle and interacts with the LOX-side flow. On the LOX side, the mean velocity shows a similar linear distribution in the entrance region closed to the LOX postbundle although it does not extend over the complete width of the racetrack because of the strong interaction with the larger LH_2-side flow.

Flow through the LOX postbundle follows the path of least resistance and this leads to the mean-flow distributions in the exit nozzle shown in Fig. 5 with a low momentum flow in the core of the exit nozzle and velocity maxima near the wall. Velocity distributions in the outlet flow of the exit nozzle, obtained by traversing in the x direction perpendicular to the inlet ducts, are sensibly symmetric under conditions with equal flow

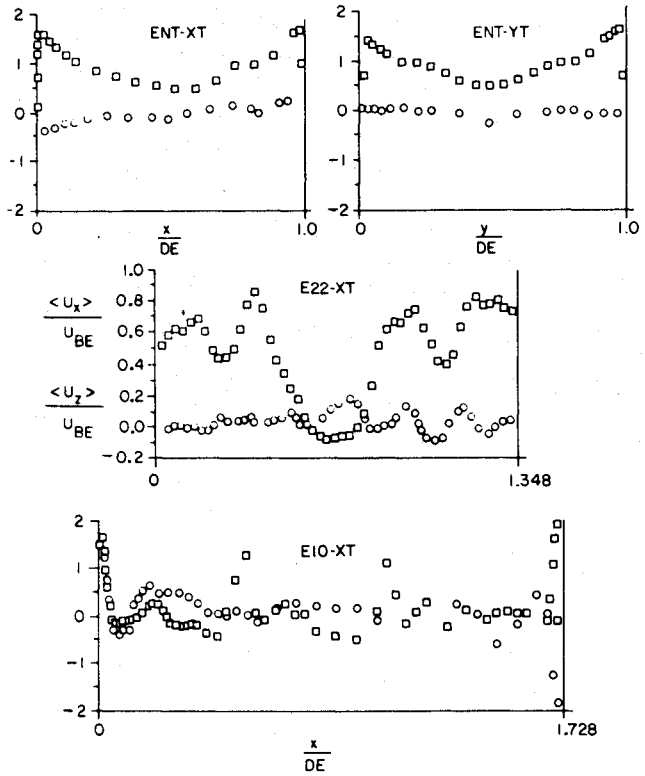

Fig. 5 Velocity distribution across exit nozzle (□ $<W>$ mean velocity; and ○ $<U>$ mean velocity).

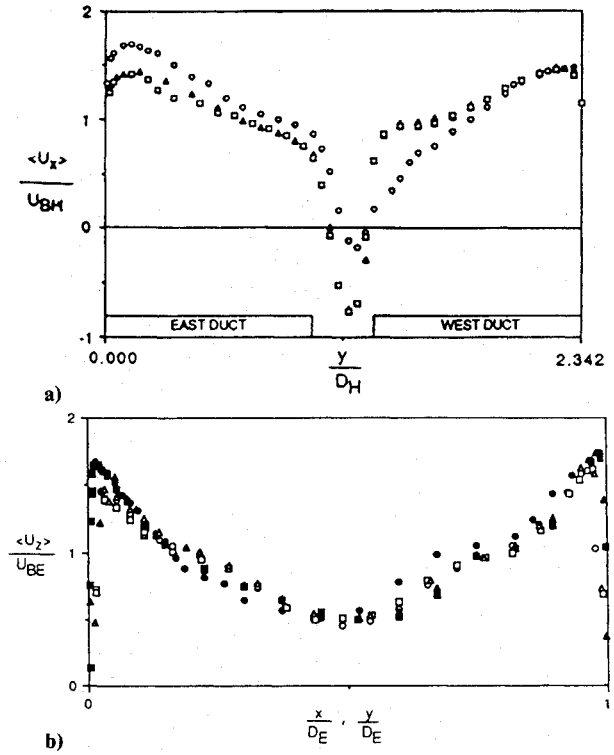

Fig. 6 Off-design conditions: a) X component of mean velocity in entrance region of racetrack (□ 70/30 LH_2/LOX flow split—equal East/West; ○ 70/30 LH_2/LOX flow split—55/45 East/West; and △ equal East/West both LH_2-side ducts—zero flow LOX-side ducts); and b) Z component of mean velocity (symbols are the same as in a) with solid symbols representing x traverse from LOX side to LH_2 side across nozzle centerline and open symbols representing y traverse perpendicular to the transfer duct axis).

from both ducts of each inlet pair. Traverses in the y direction parallel to the duct axis also provided distributions that were remarkably symmetric despite the LOX- and LH_2-side flow split of 30 and 70%, respectively, and this may be attributed to the plenum effect of the racetrack and LOX postbundle.

Off-design conditions were arranged and the measurements, which were obtained to compare with those above, are shown in Fig. 6. For a 45%/55% flow rate split between inlet ducts on the LH_2 side and equal flow rates in the LOX-side ducts, the outlet flow showed small differences from the above case primarily associated with penetration of the flow into the LOX postbundle. Similar results were obtained with the LOX-side flow off and, also, with a 5% mismatch in the LOX-side inlet duct flow rates. Of particular interest are, first, the lack of circumferential variation even with the LOX-side flow off and, second, the maxima of mean velocity near the nozzle walls. This suggests that the racetrack and LOX postbundle are an effective plenum for an even circumferential distribution of flow into the exit nozzle but that its configuration contributes to a nonuniform flow distribution in the radial direction.

V. Concluding Remarks

Flow patterns and distributions of three components of mean velocity and turbulence normal stresses have been presented in a complex model of the SSME main injector bowl. Techniques were used to match the refractive index of the fluid and the model and provided adequate optical access for laser velocimetry throughout the entire flowfield including near-wall regions where measurements were obtained within 0.02 mm (0.001 in.) of the wall. Measurement uncertainty was within acceptable limits for fluid mechanics analysis and design purposes and for the following salient conclusions about flow through the subject 32% model of the SSME main injector bowl.

1) The racetrack and LOX postbundle have an upstream influence on flow in the transfer ducts.

2) Flow in the racetrack has some characteristics of a forced vortex and there is a strong interaction of the LOX-side and LH_2-side flows.

3) The flow from the racetrack through the LOX postbundle follows the path of least resistance and this results in a nonuniform flow distribution in the radial direction across the exit nozzle.

4) Recirculating flow was present in the following locations: in the entrance regions between the inlet ducts; downstream of the sharp corners where the inlet ducts meet the injector bowl; and in the central core of the exit nozzle.

5) Results obtained at off-design conditions indicate that the racetrack and LOX postbundle effect an even circumferential distribution of flow into the exit nozzle but there is a nonuniform flow distribution in the radial direction across the exit nozzle.

The present results quantify the flow phenomena in the injector bowl and thus provide valuable fluid mechanics information that demonstrates some of the advantages of using refractive-index-matching-techniques.

Acknowledgments

Financial support from the NASA SBIR program under Contract NAS8-37410 is gratefully acknowledged. The authors thank W. Dahm and J. Heaman of NASA Marshall Space Flight Center for helpful discussions.

References

[1]Durst, F., Keck, T., and Kleine, R., "Turbulence Quantities and Reynolds Stress in Pipe Flow of Polymer Solutions," *Proceedings of the 6th Symposium on Turbulence in Liquids,* Springer-Verlag, New York, Sept. 1979, pp. 55–64.

[2]Edwards, R. V., and Dybbs, A., "Refractive-Index-Matching for Velocity Measurements in Complex Geometries," *TSI Quarterly,* Vol. 10, No. 4, 1984, pp. 3–11.

[3]Horjay, M., and Leuckel, W., "LDA Measurements of Liquid Swirl Flow in Converging Swirl Chambers with Tangential Inlets," *Proceedings of the 2nd International Symposium on Applications for Laser Anemometry to Fluid Mechanics,* Superior Technico, Lisbon, Portugal, July 1984, pp. 11.4.1–11.4.7

[4]Nouri, J. M., Whitelaw, J. H., and Yianneskis, M., "An Investigation of Refractive-Index-Matching of Continuous and Discontinuous Phases," *Proceedings of the 3rd International Symposium on Applications of Laser Anemometry to Fluid Mechanics,* Superior Technico, Lisbon, Portugal, July 1986, pp. 4.4.1.–4.4.6.

[5]Thompson, B. E., Vafidis, C., and Whitelaw, J. H., "Velocimetry with Refractive-Index Matching for Complex Flow Configurations," Scientific Research Associates, Inc., Contractor Rept. R87-900072-F, Glastonbury, CT, Aug. 1987.

[6]Yianneskis, M., Tindal, M. J., and Paul, G. R., "The Application of Laser Anemometry to the Study of Flows Inside Engine Diesel Inlet Ports," *Proceedings of the 3rd International Symposium on Applications of Laser Anemometry to Fluid Mechanics,* Superior Technico, Lisbon, Portugal, July 1986, pp. 7.5.1–7.5.5.

[7]Tindal, M. J., Cheung, R. S., and Yianneskis, M., "Velocity Characteristics of Steady Flows Through Engine Inlet Ports and Cylinders," Society of Automotive Engineers, Paper 880383, Warrendale, PA, Feb. 1988.

[8]Elphick, I. G., Martin, W. W., and Currie, I. G, "Application of LDA to High Reynolds Number Cross Flow," *Proceedings of the International Symposium on Application of Laser Anemometry to Fluid Mechanics,* Superior Technico, Lisbon, Portugal, July 1982, pp. 15.1.1.–15.1.12.

[9]Nouri, J. M., "Single and Two-Phase Flows in Ducts and in a Stirred Reactor," Ph.D. Dissertation, Fluids Section, Mechanical Engineering Dept., Imperial College, Univ. of London, London, Feb. 1988.

[10]Liu, C. H., Nouri, J. M., Thompson, B. E., Tse, D. G. N., and Whitelaw, J. H., "Two-Phase Flow Measurements with Refractive-Index-Matching Techniques," Scientific Research Associates, Inc., Contractor Rept. 900072-89-T4, Glastonbury, CT, June 1989.

[11]Nouri, J. M., Whitelaw, J. H., and Yianneskis, M., "Particle Motion and Turbulence in Dense Two-Phase Flows," *International Journal of Multiphase Flow,* Vol. 13, No. 4, pp. 729–739.

[12]Nouri, J. M., Whitelaw, J. H., and Yianneskis, M., "A Refractive-Index-Matching Technique for Solid/Liquid Flows," *Laser Anemometry in Fluid Mechanics,* Vol. 3, No. 2, 1988, pp. 335–346.

[13]Nouri, J. M., "Turbulent Flow of Moderately Dense Particles Suspensions in a Stirred Reactor," Mechanical Engineering Dept., Imperial College, Rept. FS/87/05, London, Jan. 1987.

[14]Yianneskis, M., and Whitelaw, J. H., "Velocity Characteristics of Pipe and Jet Flows with High Particle Concentration," Mechanical Engineering Dept., Imperial College, Rept. FS/83/22, London, April 1983.

[15]Taylor, A. M. K. P., and Whitelaw, J. H., "Velocity Characteristics in the Turbulent Near Wakes of Confined Axisymmetric Bluff Bodies," *Journal of Fluid Mechanics,* Vol. 139, No. 1, 1984, pp. 391–416.

[16]Thompson, B. E., and Vafidis, C., "A Special-Purpose Laser Velocimeter for SSME Water Flow Models of Rocket-Engine Configurations," Scientific Research Associates, Inc., Rept. R86-900038-F, Glastonbury, CT, Aug. 1986.

[17]Khezzar, L., Varfidis, C., and Whitelaw, J. H., "LDV Measurements of the Flow in the Hot Gas Manifold Pilot Model of the Space Shuttle Main Engine," Mechanical Engineering Dept., Imperial College, Rept. FS/87/37, London, Oct. 1987 (revised Jan. 1988).

[18]Thompson, B. E., Senaldi, J., Vafidis, C., Whitelaw, J. H., and McDonald, H., "Measurements in a Model of the SSME Main Injection Bowl," Scientific Research Associates, Inc., Contractor Rept. R89-900072-T2, Glastonbury, CT, June 1989.

Clark H. Lewis
Associate Editor